Journal of Japan Association for Earthquake Engineering, Vol. 18, No. 3, 2018

OBSERVATION OF MICROTREMOR IN KATSUYAMA BASIN, FUKUI PREFECTURE CARRIED OUT THROUGH THE MICROTREMOR RESEARCH CAMP

Michihiro OHORI[1], Yuta ASAKA[2], Hiroki AZUMA[2], Shigeki ADACHI[2], Masaki ITO[2], Yoshinobu IWANAMI[2], Taishi UENO[2], Yuki URATANI[2], Yusuke OISHI[2], Masaaki OHBA[2], Takuo OKAMOTO[2], Shohei KANEKO[2], Nobuaki KITAMURA[2], Haruki KITAMURA[2], Satoshi KURITA[2], Keisuke KOJIMA[2], Fumika SATO[2], Koki TATSUTA[2], Shohei NAITO[2], Sho NAKAI[2], Toshiki NAKAI[2], Tatsuya NOGUCHI[2], Koji HADA[2], Takumi HAYASHIDA[2], Shigeo HIGUCHI[2], Gen FURUYA[2], Naoki MAEDA[2], Tomohiro MIZUNO[2], Masashi MIYAZAKI[2], Shinichiro MORI[2], Masahiro MORITA[2], Koji YAMADA[2], Masayuki YAMADA[2], Hidekazu YAMAMOTO[2], Shohei YOSHIDA[2], Masaho YOSHIDA[2] and Hiroyuki FUJIWARA[3]

[1] Member, Secretary General of MRC, Dr. Eng.
[2] Microtremor Research Camp (MRC, Bido-no-Kai (in Japanese))
3 Member, President of MRC, Dr. Sci.

ABSTRACT: The eighth meeting of the Microtremor Research Camp (MRC) was held in Ohno City, Fukui Prefecture from September 30th to October 2nd in 2016, and MRC carried out microtremor measurements in the Katsuyama Basin, which is constituted by deposits of the Kuzuryu River. These measurements consist of microarray measurements at 25 sites and single-point measurements at 67 sites. This paper reports the outline of these measurements and presents the distribution of predominant frequencies in the basin obtained by the analysis of horizontal-to-vertical spectrum ratio at single-point measurement sites. As a result, the large differences in the distribution of predominant frequencies and peak spectral amplitudes between the Quaternary terrace deposits and alluvial deposits are clarified.

Key Words: Microtremor, Katsuyama Basin, Horizontal-to-vertical spectrum ratio, Microarray measurement, Terrace deposit

1. INTRODUCTION

The Katsuyama Basin is located in Katsuyama City, Fukui Prefecture, where a fluvial terrace has developed along the banks of the Kuzuryu River. In this area, geological information for site amplification is very limited and microtremor surveys have not been reported yet for both array measurements[1),2)] and single-point observations.[3)] In this article, we describe microtremor measurements in this area and report on the spatial distribution of peak frequencies and peak

amplitudes from the H/V spectrum ratios. We consider that our results and dataset provide useful information for seismic microzonation in future earthquake disaster assessments.[4)]

2. THE EIGHTH MEETING OF THE MICROTREMOR RESEARCH CAMP (MRC)

Microtremor measurements and preliminary analyses were conducted as the main activity during the 8th MRC[5)] held from September 30 to October 2, 2016. On September 30, we conducted microtremor measurements in the Katsuyama Basin in the daytime. We also conducted huddle testing after field measurements (Photo 1(a)). At nighttime, we organized the observed data at a hotel in Ohno City, next to Katsuyama City (Photo 1(b)). On October 1, we had a seminar for microtremor surveys in the daytime and conducted data analyses at nighttime. On October 2, we resumed the seminar for the whole day.

3. OVERVIEW OF THE GEOLOGICAL CHARACTERISTICS OF THE KATSUYAMA BASIN

Katsuyama City[6)] is located in the northeastern part of Fukui Prefecture (Fig. 1) and lies in the middle stream of the Kuzuryu River, the largest river in this prefecture. On a geological map[6)] of the area in and around Katsuyama City (Fig. 2), the Hida metamorphic rocks can be seen and are considered to be the oldest continental bedrock in the Japan islands. We can also see the Tetori Group, which contains a

(a) (b)

Photo 1 Snapshot during the 8th MRC. (a) Huddle tests. (b) Desktop study to identify peaks of the H/V spectrum ratios.

Fig. 1 Map showing location of Katsuyama City[6)].

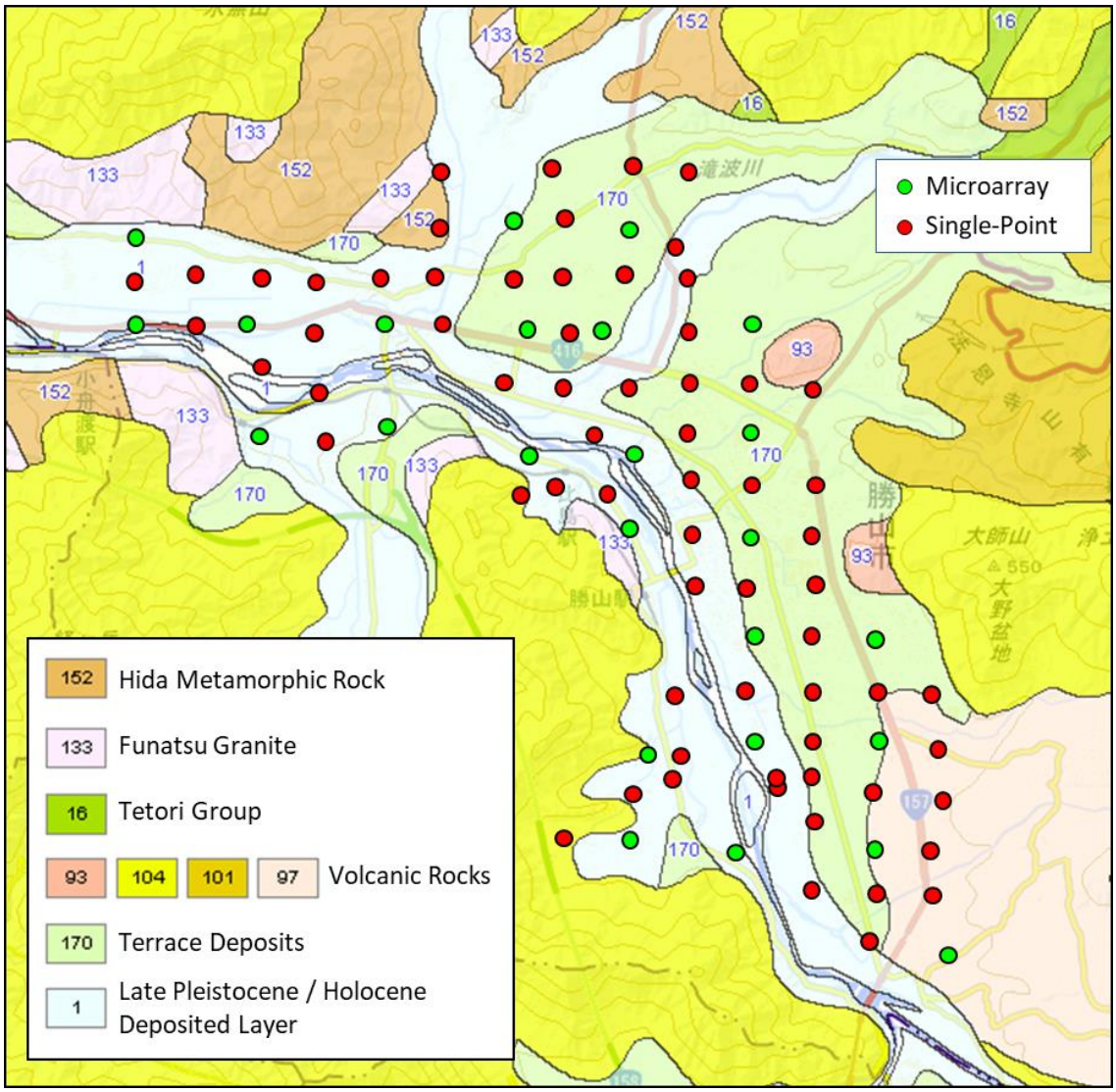

Fig. 2 Map showing surface geology in and around Katsuyama Basin. (Slightly modified from "Seamless Digital Geological Map of Japan (1:200,000)" with locations of microtremor measurements)

hundred-million-year-old dinosaur fossil. Volcanic rocks and volcanic sediments, supplied by volcanic activities a million years ago[8] in the surrounding mountains, such as Dainichisan, Hoonjiyama, Kyogatake and others, are distributed in the area. Katsuyama City is surrounded by mountains about a thousand meters high, where the Kuzuryu River has wandered for a long time and a fluvial terrace and valley plains have developed along its banks.[9] Several branches flowing into the Kuzuryu River have also developed alluvial fans that are classified as terrace deposits.[9]

The Fukui Plain is located 20 km westward from the Katsuyama Basin and its dimensions are 10–16 km east–west and 27 km north–south. In and around the Fukui Plain, energetic studies[10–12] have previously been carried out by Yasui and Kojima, who performed microtremor measurements to estimate the S-wave velocity structure. Some authors also conducted joint microtremor measurements as an activity of the 3rd MRC held at Fukui City in 2011.[5] The Ohno Basin is located south of Katsuyama Basin on the upstream side of the Kuzuryu River. Kojima[13] conducted microtremor measurements and estimated the S-wave velocity model for the Ohno Basin. Eiheiji is a town located west of Katsuyama Basin on the downstream side the Kuzuryu River. The KiK-net station of FKIH01, operated by the National Research Institute for Earth Science and Disaster Resilience (NIED), is located on the fluvial terrace of the right bank right bank of the Kuzuryu River in Eiheiji and is recognized

as an important reference site for site amplification evaluations in Fukui Prefecture. To better understand the site's response characteristics, microtremor measurements were performed at the Eiheiji observatory station and in the nearby area,[14),15)] but for Katsuyama City no microtremor surveys of array measurements[1),2)] or single-point observations[1)] have been made. Katsuyama Basin is considered to be a blank area in terms of microtremor measurements, although most other areas in the Fukui Prefecture have been well investigated.

4. MICROTREMOR MEASUREMENTS

Microtremor measurements were conducted on September 30, 2016. We separated into 12 teams, each team consisting of 1–4 persons, and performed microtremor observations at 92 sites: single-point measurements at 67 sites and 0.6 m-radius microarray measurements at 25 sites (Table 1). Among the 12 teams, three traveled by car for array measurements, six walked for single-point measurements, and the remaining three traveled by car for single-point measurements. We made a base camp at a parking area west of Katsuyama Station and prepared additional equipment, maps, etc., for emergency. The observed sites were distributed in an area 7 km east–west by 8 km north–south with a resolution of 500 m. The location of sites was determined to be the roadside by using an aerial photograph. A seamless map, as well as printed maps, were prepared by mobile terminals (Fig.3). For most participants, it was their first visit to the Fukui Prefecture, much less Katsuyama City. All teams could check their location at any time, so they had no problems with field observations and successfully accomplished their mission. Photo 2 is a snapshot of an observation.

Table 1 The seismometers used by each team.

No.	Seismometers	Site Names												
1	JU310	T021	T023	T027	T030	T031	T032							
2	JU310	T029	T036	T038	T040	T041								
3	JU310	T025	T026	T028	T033	T034	T035							
4	JU310	T016	T017	T018	T019	T022	T024							
5	JU310	T005	T006	T007	T008	T013	T015							
6	JU310	T037	T043	T045	T046	T047	T048							
7	JU210	T044	T053	T055	T056	T057	T058	T102	T115	T116	T117	T118		
8	JU210	T002	T003	T004	T009	T010	T011	T012	T066	T067	T068	T074	T076	
9	Lennartz LE-3Dlite & LS-8000SH (logger)	T087	T089	T090	T091	T092	T096	T097	T098	T099				
10	JU210×4	A002	A003	A004	A005	A006	A007	A009	A010	A011	A012	A015	A019	A029
11	JU210×4	A035	A036	A037	A038	A041	A042							
12	JU410×3, HS-1×4+HKS9700 (logger)	A013	A014	A017	A018	A021	A022							

[Note] Microtremor sites (site names starting with "T" correspond to single-seismometer sites for H/V spectrum ratios; site names starting with "A" correspond to sites for microarray measurements).

(a) Large scale map (b) Example map of close-range view

Fig. 3 Seamless map for mobile terminals. (Background map is from Google Maps.) (●Single-point measurements, ▲Array measurements.)

For most of measurements, we used ten sets of JU210, six sets of JU310, three sets of JU410, all of which are portable three-component acceleration seismometers made by Hakusan Corporation. We also used four sets of vertical velocity seismometers (HS-1, made by Oyo Keisoku Corporation) connected with data loggers (HKS9700, made by Keisoku Giken Corporation) and a set of three-component velocity seismometers (LE-3D lite, made by Lennartz) with a data logger (DATAMARK LS-8000SH, made by Hakusan Corporation). Note that the huddle test verified that all seismometers had no significant differences between 0.2 and 10 Hz.

For single-point measurements, we used JU210 and JU310. For microarray measurements, we used four sets of JU210, installing one at the center and spacing the other three equally on the circumference of a 0.6 m-radius circle. For six array sites (A013, A014, A017, A018, A021, A022), four sets of HS-1s and three sets of JU410s were used together. HS-1s were used for 0.6 m-radius microarray measurements and JU410s were used for the 5 m array with an irregular shape. The seismometers used by all teams are summarized in Table 1. We assigned at least one experienced observer to each team. Before field observations, all teams were instructed as follows.

(1) Sensors should be directed in the northerly direction with a compass.
(2) The sampling frequency should be set to 100 Hz.
(3) Observations should be carried out more than 15 min at each site to make more than 15 one-minute WIN-format files.
(4) During observations, sensors should be protected with wind covers.
(5) Pictures around sites should be taken from short and long distance.
(6) Field notes should be filled out as shown in Fig. 4.

5. RESULTS OF MICROTREMOR MEASUREMENTS

We conducted microtremor measurements at 92 sites in the Katsuyama Basin, of which 67 sites were single-point measurements and 25 sites were 0.6 m-radius microarray measurements (Fig. 5). The coordinates (latitude and longitude) are summarized in Table 2. In microarray measurements, extremely small arrays were deployed, so we expect that in future work the data will be analyzed by the centerless circular array method proposed by Cho and others[16] to estimate the shallow surface structure up to 10–100 m in depth. In this article, we report preliminary results obtained during the camp: peak frequencies and corresponding amplitudes of horizontal-to-vertical (H/V) spectrum ratios.

To calculate the H/V spectrum ratio of each site, we first searched for relatively silent segments from whole observed data of 15 min and finally selected five segments with data length 40.96 s. To smooth spectral amplitudes, we applied the Parzen window with 0.2 Hz width to both horizontal and vertical spectra. The H/V spectrum ratios from five segments were averaged. The horizontal spectral amplitudes were obtained from the geometric mean of spectra of two components.

Photo 2 Snapshot during microtremor measurements (A038, Distant view).

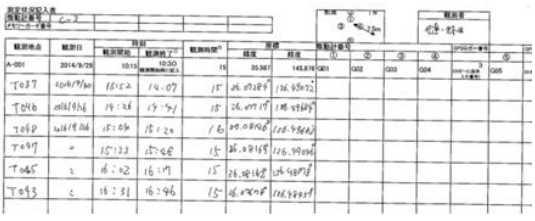

Fig. 4 Example field note.

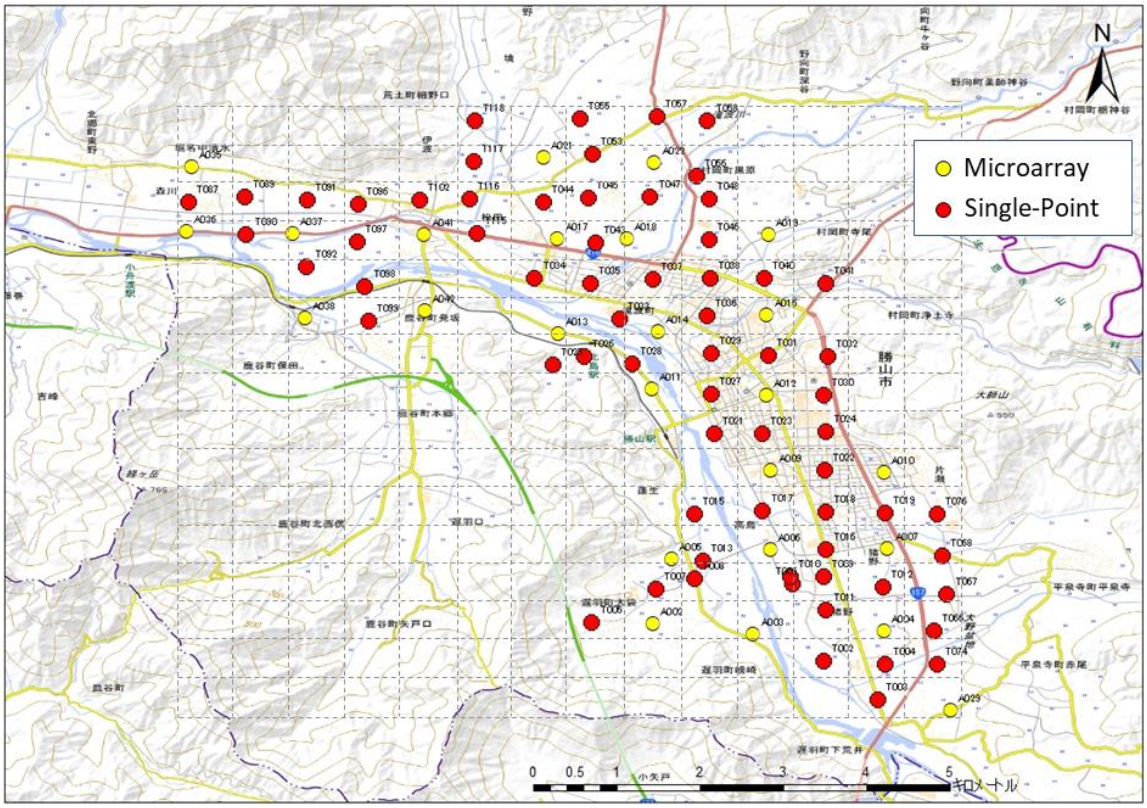

Fig. 5 Map showing location of microtremor measurements. (Background map is from pale color map from Geographical Survey Institute. Grids of broken lines are corresponding to Figs 6 and 7.)

Table 2 Summary of observed site locations.

Site Name	Longitude (°)	Latitude (°)	Site Name	Longitude (°)	Latitude (°)	Site Name	Longitude (°)	Latitude (°)
A002	136.49069	36.03577	T008	136.49528	36.04056	T043	136.48457	36.07678
A003	136.50159	36.03457	T009	136.50917	36.04083	T044	136.47891	36.08117
A004	136.51567	36.03495	T010	136.50556	36.04083	T045	136.48378	36.08162
A005	136.49277	36.04271	T011	136.50944	36.03722	T046	136.49684	36.07717
A006	136.50340	36.04376	T012	136.51556	36.03972	T047	136.49046	36.08169
A007	136.51607	36.04387	T013	136.49611	36.04250	T048	136.49683	36.08146
A009	136.50349	36.05223	T015	136.49528	36.04750	T053	136.48422	36.08634
A010	136.51567	36.05205	T016	136.50940	36.04370	T055	136.48286	36.09019
A011	136.49062	36.06107	T017	136.50260	36.04790	T056	136.49543	36.08402
A012	136.50298	36.06031	T018	136.50940	36.04780	T057	136.49117	36.09037
A013	136.48049	36.06701	T019	136.51580	36.04770	T058	136.49664	36.08989
A014	136.49127	36.06726	T021	136.49738	36.05621	T066	136.52111	36.03500
A015	136.50304	36.06903	T022	136.50930	36.05230	T067	136.52250	36.03889
A017	136.48044	36.07719	T023	136.50251	36.05617	T068	136.52194	36.04306
A018	136.48793	36.07722	T024	136.50940	36.05640	T074	136.52139	36.03139
A019	136.50317	36.07772	T025	136.47994	36.06368	T076	136.52139	36.04750
A021	136.47893	36.08597	T026	136.48328	36.06455	T087	136.44058	36.08116
A022	136.49088	36.08542	T027	136.49704	36.06049	T089	136.44663	36.08175
A029	136.52290	36.02644	T028	136.48844	36.06373	T090	136.44683	36.07765
A035	136.44090	36.08497	T029	136.49700	36.06485	T091	136.45339	36.08139
A036	136.44038	36.07798	T030	136.50914	36.06039	T092	136.45335	36.07421
A037	136.45186	36.07781	T031	136.50317	36.06463	T096	136.45897	36.08094
A038	136.45314	36.06870	T032	136.50962	36.06454	T097	136.45877	36.07692
A041	136.46605	36.07769	T033	136.48712	36.06857	T098	136.45965	36.07202
A042	136.46613	36.06942	T034	136.47798	36.07301	T099	136.46005	36.06839
T002	136.50917	36.03167	T035	136.48401	36.07238	T102	136.46558	36.08134
T003	136.51500	36.02750	T036	136.49662	36.06892	T115	136.47172	36.07776
T004	136.51583	36.03139	T037	136.49072	36.07284	T116	136.47094	36.08148
T005	136.48417	36.03583	T038	136.49687	36.07291	T117	136.47144	36.08552
T006	136.50583	36.04000	T040	136.50272	36.07296	T118	136.47150	36.08990
T007	136.49111	36.03944	T041	136.50936	36.07245			

Next, we investigated the H/V spectrum ratios and determined the peak frequencies and corresponding amplitudes. For efficiency in studies of this kind, we separated into ten groups of three or more persons. To avoid errors caused by different interpretation of different persons, peak determinations were done carefully with unanimous consensus of all team members. When peaks in the H/V spectrum ratios were not clear and several peaks were detected, information about topography and geology was taken into account. In compilation of peak frequency results, cross-checks were made. Peak frequencies higher than 10 Hz were truncated at 10 Hz. Figs 6 and 7 show the spatial distribution map of peak frequencies and their corresponding amplitudes, respectively. In these figures, only results derived from clear peaks were plotted. Peak frequencies higher than 10 Hz were plotted as 10 Hz in Fig. 6, but their corresponding amplitudes were omitted in Fig. 7. From Fig. 6, it seems that the peak frequency tends to be relatively low in the central area of the basin covered with thick sediments, and relatively high near the basin's edge with thin sediments. In contrast, in the northern part of the observed area (upper central portion of the map), the peak frequency is relatively high (in purple), although it is located in the central area of the basin with thick sediments. In the southern part (lower right portion of the map), the peak frequency is higher than 5 Hz (in light blue). As can be observed in Fig. 7, peak amplitudes generally tended to be large in the central area of the basin and small near the basin's edge, although the small amplitude (in yellow) is locally seen in the middle of the basin (middle right).

6. DISCUSSION

6.1 Comparison of results from mocirotremor observation with AVS30 and amplification from geomorphologic classification

Using the NIED's "Japan Seismic Hazard Information Station" (J-SHIS) database,[17] microtremor sites are plotted on a map of geomorphologic classification[18),19] in and around the Katsuyama Basin (Fig. 8). Using the J-SHIS database, the average S-wave velocity from the surface to a depth of 30 m (AVS30[20]) and the amplification factor[21] of the maximum velocity between the surface and top of the engineering bedrock with the S-wave velocity of 400 m/s were extracted. In Fig. 9, peak frequencies and corresponding amplitudes derived from microtremor measurements are compared with the AVS30 and amplification factors. Based on the assumption of a simplified soil structure composed of a soft layer and bedrock, a positive correlation was expected between the peak frequencies and AVS30, and between the peak amplitudes and amplification factors. Similarly, negative correlations were expected between the peak frequencies and peak amplitudes, and between the peak amplitudes and AVS30.[4] However, such expected correlations were not found, as Fig. 9 shows. The AVS30 and amplification factors for each type of geomorphologic classification seem to be constant despite changes in peak frequencies and corresponding amplitudes. This tendency may suggest that the soil characteristics in this area are not considered enough in the evaluation of AVS30 and the amplification factor determined by geomorphologic classification. In other words, it may imply the limit of the current empirical evaluation method for the AVS30 and amplification factors, whose parameters are composed of altitude, slope, distance between targeted site and nearby mountain or hill.

The 92 sites for which we calculated the H/V spectral ratios were classified into five geomorphologic categories, as follows: two sites were mountain, 11 were volcanic foot slope, 40 were gravelly terrace, 21 were valley bottom lowland, and 18 were alluvial fan. Matsuoka and others[22] pointed out that the deviation between the data and estimation of AVS30 was relatively large for valley bottom lowland compared with other categories. They[22] explained that "along large rivers, soil conditions upstream close to a mountainous area are different from those downstream. The former valley is narrow, and hard bedrock forming the mountain and/or terrace appears at a shallow depth. On the other hand, the latter valley is wide, and the bedrock is lying in a deep portion. Therefore, the AVS30 of the valley bottom lowland has a large deviation." As for the AVS30 for gravelly terrace, they also pointed out the large discrepancies between data and estimation. They[22] describe, "a gravelly terrace is classified into two types of geomorphologic classification: river terrace (along the river) and

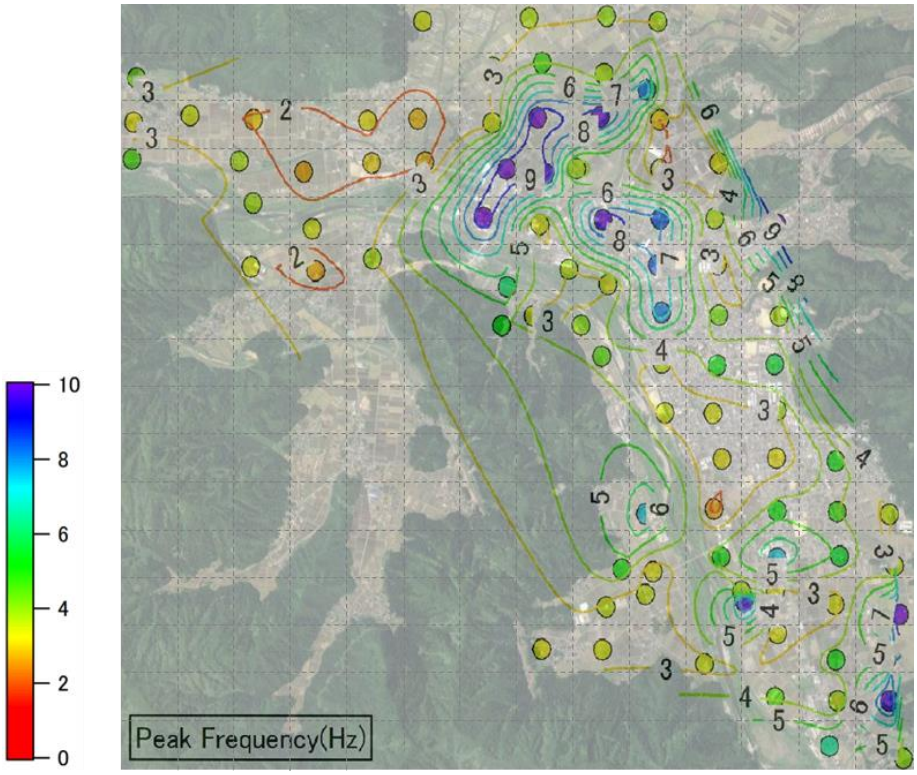

Fig. 6 Map showing peak frequencies derived from H/V spectrum ratios. (Background map is from Google Maps.)

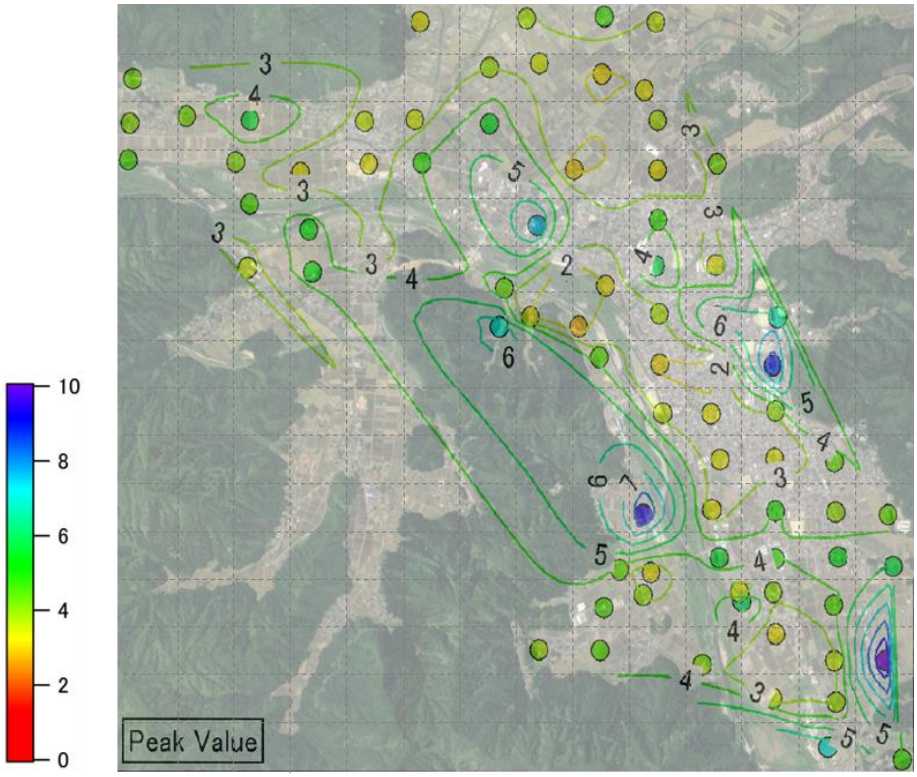

Fig. 7 Map showing peak amplitudes derived from H/V spectrum ratios. (Background map is from Google Maps.)

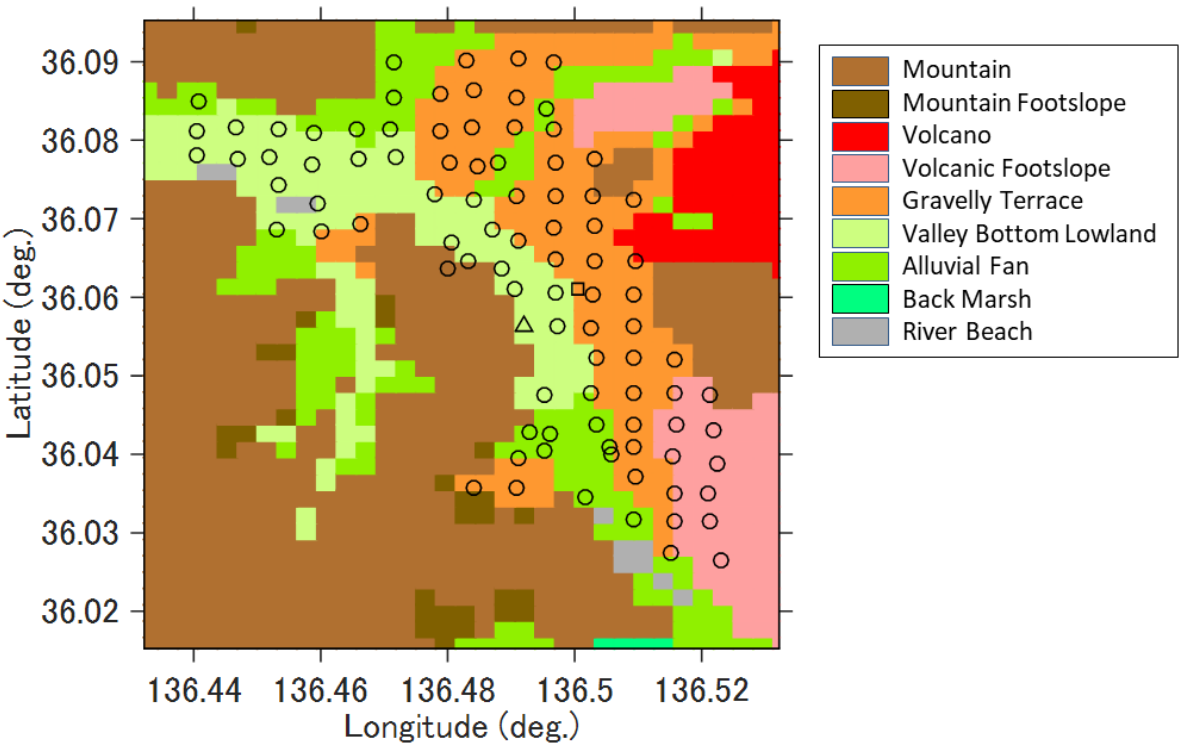

Fig. 8 Map showing the geomorphologic classification[18),19)] and microtremoer measurement sites in Katsuyama Basin. (○ : Observatory Sites, △ : Katsuyama Railway Station, □ : Katsuyama City Hall)

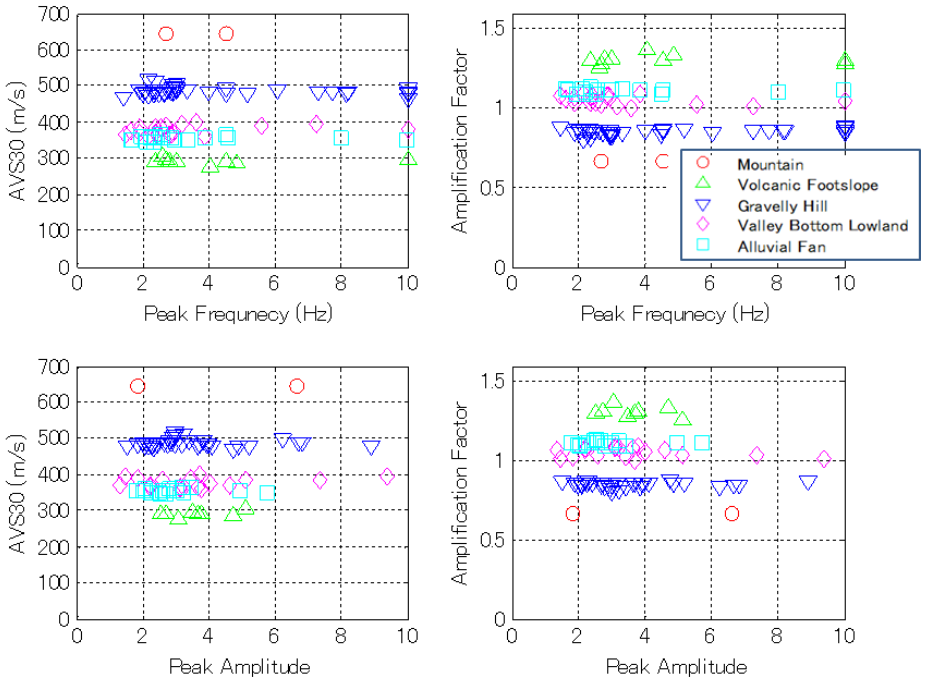

Fig. 9 Relationship among peak frequencies, peak amplitudes from H/V spectrum ratios, and AVS30, amplification factors from Geomorphologic Classification.

liftup of marine terrace and alluvial fan, so the difference in the formation process may lead to the difference in AVS30." As most of sites in this study were valley bottom lowland and gravelly terrace, it was difficult to estimate AVS30 based on geomorphologic classification. We therefore emphasize that the high-density observations in this study will be basic data useful for improving estimation of AVS30 and amplification factors, enhancing the accuracy of the seismic shake map of Katsuyama Basin during future earthquake scenarios, and complementing the J-SHIS.

6.2 Problems in collaboration for data analyses

After the joint observations, we split into ten teams of three or four and determined the peak frequencies and amplitudes of the H/V spectrum ratios. Although each team needed a person who was very experienced in peak determination of H/V spectrum ratios, attendants naturally separated into teams, and some teams lacked such a person. Therefore, such teams could not reliably determine spectral peaks and had large deviations. Fig. 10 shows examples of the results that may have caused potential errors in peak determinations for the H/V spectrum ratios. In this figure, the finally determined peak frequencies and corresponding amplitudes are denoted by open circles in red, those potentially judged by different persons are denoted by downward arrows in green. In particular, sites showing low correlation between peak frequency and AVS30 may involve problems of this kind.

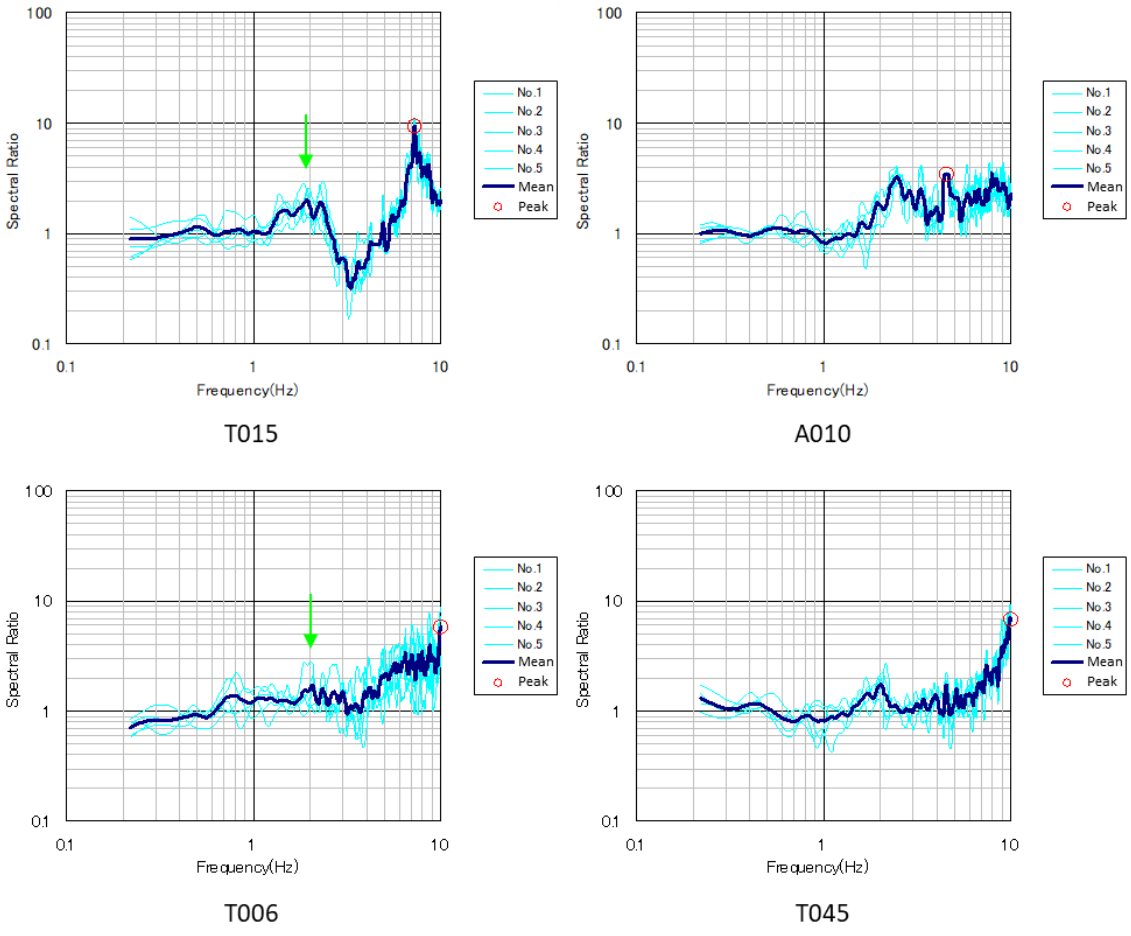

Fig. 10 Example of H/V spectrum ratios: cases potentially identifying different peaks.(Final peak frequency and corresponding amplitudes are denoted by ○, potential peak frequency and corresponding amplitudes by person to person are denoted by ↓.)

It should be noted that the multiple peaks found in the H/V spectrum ratios may be useful as geological information. For example, for the Fukui Plain, more higher density microtremor measurements showed that multiple peaks in the H/V spectrum ratios were commonly found in the plain and changed continuously. It is considered that a spectral peak in the lower frequency range provides information for the deep underground structure, and a peak in the higher frequency range provides information about the shallow structure[11),12)]. To better understand soil characteristics of a targeted area and to obtain more reliable geological information of a river terrace and valley bottom lowland located in the middle stream, a 500 m grid size is too wide for measurements; finer grid observation should be conducted in the next time.

7. CONCLUSIONS

We conducted microtremor measurements in Katsuyama Basin on September 30, 2016. In this report, we give an overview of the joint observations, data organization, and preliminary analyses undertaken so as to publish our data as soon as possible. To estimate the S-wave velocity structure for a seismic hazard map, further studies including array data analyses are required. We will also continue our MRC activity to improve understanding and sharing of microtremor measurements and analyses. The data reported here is available by request from the first author.

ACKNOWLEDGMENT

These joint microtremor observations were held during the 8th annual meeting of the MRC. We are sincerely grateful to the founding members for their longtime efforts and support of the MRC.

REFERENCES

1) Fujiwara, H.: Development of integrated geophysical and geological information database, *Proc. 3rd Symposium of Integrated Geophysical and Geological Information Database (An Interim Report)*, pp. 5-14, 2009. (in Japanese)
2) Asano, K., Iwata, T., Miyakoshi, K., and Ohori, M.: Study on Underground Velocity Structure Model in the Kaga Plain and the Ochigata Plain using Microtremor Observations, *Journal of Japan Earthquake Engineering Association*, Vol. 15, No. 7, pp. 194-204, 2015. (in Japanese)
3) Kojma, K.: Personal Communication.
4) Yamada, M., Hara, T., Kitamura, K., Takezawa, K., Hada, K., and Yagi, S.: Study on Utilization of Microtremor Data for Accurate Shaking Hazard Maps, *Journal of Institute of Social Safety Science*, No. 22, March, #4, 10p., 2014. (in Japanese)
5) Senna, S.: Sharing of the Knowledge and Data about Microtremor Observation: A Report of Activity of 'The Party for Microtremor', *Proceedings of the 131st SEGJ Conference*, pp. 224-225, 2014. (in Japanese)
6) Fukui Prefecture: http://www.pref.fukui.jp/doc/zaisei/takarakuji/uribaitirann.html (in Japanese, last accessed in November 10, 2016).
7) National Institute of Advanced Industrial Science and Technology (ed.): *Seamless Digital Geological Map of Japan (1:200,000)*, https://gbank.gsj.jp/seamless/seamless2015/2d/. (in Japanese, last accessed in May 29, 2015)
8) Geological Socoiety of Japan (ed.): *Regional Geology of Japan: (4) Chubu Region*, Asakura Publishing, Co. Ltd., 564p., 2006. (in Japanese)
9) Fukui Prefecture: *Geological Map of Fukui Prefecture: 2010 Edition*, Fukui Prefectural Public Corporation of Construction Technology, 173p., 2010. (in Japanese)
10) Yasui, Y., Hashimoto, Y., Noguchi, T., and Kagawa, T.: Reevaluation of Existing Ground

Structure Model gained through Microtrmor Array Method by using Fundamental Properties of Model surveied through H/V Spectrum - On Ground Structure of Fukui Plain -, *Journal of Japan Society of Civil Engineers*, Vol. 68, No. 4, pp. I_305-I_314, 2012. (in Japanese)
11) Kojima, K, and Moto, K.: Estimation of S-wave Velocity Structure of Fukui Plain based on Microtrmoer Array Observation, *Journal of Japan Society of Civil Engineers*, Vol. 68, No. 1, pp. 98-109, 2012. (in Japanese)
12) Kojima, K. and Yasui. Y.: Estimation of S-wave Velocity Structure Down to the Seismic Bedrock of Fukui Plain based on Microtremor Observation, *Journal of Japan Society for Natural Disaster Science*, Vol. 33, No. 4, pp. 359-374, 2015. (in Japanese)
13) Kojima, K.: Estimation of S-wave Velocity Structure of Ohno Basin based on Microtremor Observation, *Journal of Japan Society Engineering Geology*, Vol. 55, No. 1, pp. 28-37, 2014. (in Japanese)
14) Yasui, Y. and Noguchi, Y.: Velocity Structures of K-NET Fukui Station and KiK-net Eiheiji Station, *Proceedings of the 2004 Annual Meeting, Japan Association for Earthquake Engineering*, pp. 328-329, 2004. (in Japanese)
15) Suzuki, H. and Ohba, M.: Microtremor Observation near K-K-net Eiheiji Station for Estimation of Seismic Ground Motion, *Proceedings of the 131st SEGJ Conference*, pp. 26-29, 2014. (in Japanese)
16) Cho, I.: *Microtremor Analysis Codes BIDO*, https://staff.aist.go.jp/ikuo-chou/bidodl.html. (last accessed in November 10, 2016)
17) National Research Institute for Earth Science and Disaster Prevention: *Japan Seismic Hazard Information Station*, http://www.j-shis.bosai.go.jp/. (in Japanase, last accessed in November 10, 2016)
18) Wakamatsu, K. and Matsuoka, M.: Development of a Nationwide 7.5-Arc-Second Japan Engineering Geomorphologic Classification Map and its Usage, *Bulletin of JAEE*, Vol. 18, No. 1, pp. 33-38, 2013. (in Japanese)
19) Wakamatsu, K. and Matsuoka, M.: Nationwide 7.5-Arc-Second Japan Engineering Geomorphologic Classification Map and Vs30 Zoning, *Journal of Disaster Research*, Vol. 8, No. 5, pp. 904-911, 2013.
20) Matsuoka, M. and Wakamatsu, K.: Site amplification capability map based on the 7.5-arc-second Japan engineering geomorphologic classification map, National Institute of Advanced Industrial Science and Technology, Intellectual Property Management No. H20PRO-936, 2008. (in Japanese)
21) Fujimoto, K. and Midorikawa, S.: Relationship between Average Shear-Wave Velocity and Site Amplification Inferred from Strong Motion Records at Nearby Station Pairs, *Journal of Japan Earthquake Engineering Association*, Vol. 6, No. 1, pp. 11-22, 2006. (in Japanese)
22) Masashi, M., Wakamatsu, K., Fujimoto, K., and Midorikawa, S.: Average Shear-wave Velocity Mapping using Japan Engineering Geomorphologic Classification Map, *Journal of Japan Society of Civil Engineers*, No. 794, I-72, pp. 239-251, 2005. (in Japanese)

(Original Japanese Paper Published: August, 2017)
(English Version Submitted: April 19, 2018)
(English Version Accepted: May 11, 2018)